Egyptian Journal of Petroleum (2015) 24, 27–35

HOSTED BY

ELSEVIER

Egyptian Petroleum Research Institute

Egyptian Journal of Petroleum

www.elsevier.com/locate/egyjp
www.sciencedirect.com

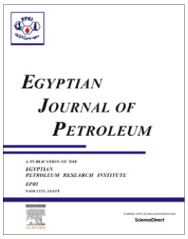

FULL LENGTH ARTICLE

# Adsorption of heavy metal ion from aqueous solution by nickel oxide nano catalyst prepared by different methods

**Amira M. Mahmoud** [a], **Fatma A. Ibrahim** [a], **Seham A. Shaban** [b,*], **Nadia A. Youssef** [a]

[a] *Faculty of Girls, Ain Shams University, Egypt*
[b] *Egyptian Petroleum Research Institute (EPRI), Egypt*

Received 13 February 2014; accepted 12 May 2014
Available online 11 April 2015

**KEYWORDS**

Adsorption;
Aqueous solution;
Heavy metal;
Nickel oxide;
Nano catalyst

**Abstract** Environmental pollution by heavy metal is arising as the most endangering tasks to both water sources and atmosphere quality today. The treatment of heavy metals is of special concern due to their recalcitrance and persistence in the environment. To limit the spread of the heavy metals within water sources, nickel oxide nanoparticles adsorbents were synthesized and characterized with the aim of removal of one of the aggressive heavy elements, namely; lead ions. Nano nickel oxide adsorbents were prepared using NaOH and oxalic acid dissolved in ethanol as precursors. The results indicated that adsorption capacity of Pb(II) ion by NiO-org catalyst is favored than that prepared using NaOH as a precipitant. Nickel oxide nanoparticles prepared by the two methods were characterized structurally and chemically through XRD, DTA, TGA, BET and FT-IR. Affinity and efficiency sorption parameters of the solid nano NiO particles, such as; contact time, initial concentration of lead ions and the dosage of NiO nano catalyst and competitive adsorption behaviors were studied. The results showed that the first-order reaction law fit the reduction of lead ion, also showed good linear relationship with a correlation coefficient ($R^2$) larger than 0.9.


## 1. Introduction

Revelation to heavy metals, even at trace levels, is harmful to human beings [1–4]. Thus, removal of undesirable metals from water sources is considered as an important task that is still threatening the environment. As the tolerable limit of lead in drinking water is 0.05 mg $l^{-1}$ [5], the presence of excess lead ions in drinking water causes severe diseases such as anemia, encephalopathy, and hepatitis. Lead ions are characterized by an eager affinity towards ligands containing thiol and phosphate groups that inhibit, in turn, the biosynthesis of heme, causing physiological damage to both the kidney and liver; similar to that of calcium. However, Pb can remain immobilized and retarded for long periods and hence it's after effects

* Corresponding author.
Peer review under responsibility of Egyptian Petroleum Research Institute.

http://dx.doi.org/10.1016/j.ejpe.2015.02.003

on the function of the human organs are detected on the metabolic disorders, it causes, but after a lag time.

Numerous methods are reported as efficient for the removal of heavy metal ions from water sources, including chemical precipitation, ion exchange, adsorption, membrane filtration and electrochemical technologies [6–11]. Among these techniques, adsorption offers flexibility in design and operation and, in many cases it generates high-quality treated effluents. In addition, owing to the reversible nature of most adsorption processes, adsorbents could be regenerated by suitable desorption processes for multiple use [12]. In addition, many desorption processes are of low maintenance cost, high efficiency, and ease of operation [13]. Therefore, the adsorption process is considered as one of the major suitable technique for heavy metals removal from water/wastewater sources.

Currently, nanosized metal oxides (NMOs), including nanosized ferric oxides, manganese oxides, aluminum oxides, titanium oxides, magnesium oxides and cerium oxides, are classified as promising adsorbents for heavy metal removal from aqueous systems [14–17]. The size and shape of NMOs are considered as the most influential factors with regard to their adsorption performance. In the present work, systematic laboratory investigations for the removal of Pb(II) ions from aqueous solutions through adsorption by nano NiO, prepared by two different precursors were performed for maximum Pb ion removal.

## 2. Materials and methodology

### 2.1. Lead ion solution adsorbate

A stock solution of Pb(II) (1000 ppm) was prepared by dissolving the calculated quantity of $Pb(NO_3)_2$ for Pb(II) in deionized water.

### 2.2. Nano NiO adsorbent

#### 2.2.1. Preparation of NiO by precipitation method

The metal hydroxide is firstly prepared by the slow addition of 0.1 M NaOH to the same volume of 0.1 M Nickel nitrate solution with vigorous stirring. The produced hydroxide precipitates are then filtered and then dried at 100 °C overnight. The dried hydroxide was then calcined at 400 °C for 2 h in order to acquire the corresponding NiO catalyst designated in the present work as ($NiO_{ppt}$).

#### 2.2.2. Preparation of NiO by organic solvent method

Solution of 1 M oxalic acid, dissolved in ethanol, was added to the same volume of 0.2 M nickel nitrate, dissolved also in ethanol solution, with vigorous stirring. The precipitate was then washed with ethanol several times until the filtrates become colorless, then finally washed with acetone and dried at room temperature. The product was then calcined at 400 °C for 1 h to acquire the corresponding NiO catalyst [18], designated in the present work as ($NiO_{org}$).

### 2.3. Chemicals

All the chemicals were of analytical-reagent grade.

### 2.3. Chemical and structural characterization apparatus

Perkin-Elmer 2380 atomic absorption spectrometer was used for the determination of lead using a flame type air/acetylene, while FT-IR spectra were obtained by Perkin Elmer 1000 with a resolution of 4 for the chemical identification of reactants and products. Philips 1390 X-ray powder diffractometer was used for structural identification and Quantachrome Corporation Autosorb-1-C/MS was used for BET surface area determination.

### 2.4. Adsorption experiments

Batch adsorption experiments of the lead ion adsorption by nano $NiO_{ppt}$ and $NiO_{org}$ adsorbents were carried out at room temperature by shaking a series of bottles each containing the desired quantity of the adsorbent in a predetermined concentration of heavy metal solution. Samples were withdrawn at different time intervals; the supernatant was separated by filtration and analyzed for remaining heavy metal content. The percent removal of heavy metal from solution was calculated by the following equation:

$$\%\text{Adsorption} = \frac{C_o - C_e}{C_o} \times 100$$

where; $C_o$ is initial concentration of heavy metal, $C_e$ is final concentration of heavy metal.

### 2.5. Adsorption isotherms

The adsorption isotherm that describes the adsorption pattern between the Pb adsorbed metal ions on the nano NiO adsorbent and the residual metal ions in the solution during the surface adsorption was conducted. Equilibrium isotherms are measured to determine the capacity of the adsorbent for metal ions. The most common types of models describing this type of system are the Langmuir and Freundlich models [19]. The adsorption capacity $q_e$ (mg/g) after equilibrium was calculated by a mass balance relationship equation as follows:

$$q_e = (C_o - C_e)\frac{V}{W}$$

where $C_o$ is the initial and $C_e$ is the equilibrium concentrations of the test solution (mg/L), $V$ is the volume of the solution (L) and $W$ is the mass of adsorbent (g).

#### 2.5.1. Langmuir model

Langmuir adsorption model is based on the assumption that the maximum adsorption corresponds to a saturated monolayer of solute molecules on the adsorbent surface. Langmuir equation can be described by the linearized form [18],

$$\frac{1}{q_e} = \left(\frac{1}{q_m k_L}\right).\left(\frac{1}{C_e}\right) + \frac{1}{q_m}$$

where, $C_e$ is the equilibrium concentration of metal ions in solution (mg/L), $q_e$ is the amount of metal ion adsorbed on adsorbents (mg/g), and $q_m$ and $k_L$ are the monolayer adsorption capacity (mg/g) and Langmuir equilibrium constant (L/mg) which indicates the nature of adsorption, respectively. The

values of $q_m$ and $k_L$ were determined graphically. A plot of $\frac{1}{q_e}$ versus $\frac{1}{C_e}$ gives a straight line of slope $\frac{1}{q_m k_L}$ and the intercept is $\frac{1}{q_m}$ which corresponds to complete monolayer coverage.

#### 2.5.2. Freundlich model

Freundlich adsorption isotherm represents the relationship between the amount of metal adsorbed per unit mass of the adsorbent $q_e$ and the concentration of the metal in solution at equilibrium. Freundlich equation can be described by the linearized form [20];

$$log\ q_e = log\ k_F + \frac{1}{n} log\ C_e$$

where $k_f$ and $n$ are Freundlich constants. The values of $k_F$ and $n$ were determined graphically. A plot of $log\ q_e$ versus $log\ C_e$ gives a straight line of slope $\frac{1}{n}$ and the intercept is $log\ k_F$.

## 3. Results and discussion

### 3.1. Characteristics of adsorbing material

#### 3.1.1. X-ray diffraction study (XRD)

Purity and crystalline structures of $NiO_{ppt}$ and $NiO_{org}$ nanoparticles were examined using powder X-ray diffraction (XRD), results of which are presented in Figs. 1 and 2. Fig. 1 indicates that the diffraction peaks are low and broad due to the small size effect and incomplete inner structure of the particle. The peak positions appearing at 2 < theta >, 37.2°, 43.22°, 63.10°, 75.20°, and 79.39 °can be readily indexed as (1 0 1), (0 1 2), (1 1 0), (1 1 3), and (0 0 6) crystal planes of the bulk NiO, respectively. All these diffraction peaks can be perfectly indexed to the face-centered cubic (FCC) crystalline structure of NiO, not only in peak position, but also in their relative intensity, which is in accordance with that of the standard spectrum (JCPDS, No. 04-0835). The XRD pattern shows that the samples are single phase and noother impurity distinct diffraction peak in addition to the characteristic peaks of FCC phase NiO. XRD patterns thus indicate highly pure NiO nanoparticles [21,22].

#### 3.1.2. FTIR analysis of the precursor

FTIR spectra of the precursor powder dried at 105 °C for 6 h are illustrated in Figs. 3 and 4 shown in transmittance percentage, several absorption peaks were observed. Figs. 3 and 4 of FTIR spectra of NiO nanoparticles show several significant absorption peaks. The broad absorption band in the region of 400–850 $cm^{-1}$ is assigned to Ni–O stretching vibration mode; the broadness of the absorption band indicates that the NiO powders are nanocrystals. Besides the Ni–O vibration, it could be seen from the same figures that the broad absorption band centered at 3357.9, 3347.4 $cm^{-1}$ is attributable to the band O–H stretching vibrations and the weak band near 1621.8, 1616.6 $cm^{-1}$ assigned to H–O–H bending vibration mode was also presented due to the adsorption of water in air when FTIR sample disks were prepared in an open air [23].

#### 3.1.3. Thermo gravimetric analysis of the precursor

The thermal decomposition of the precursors from ambient temperature to 1000 °C under a nitrogen atmosphere is shown in Fig. 5, both the thermogravimetry curves TGA (wt% loss) and differential thermogravimetry curves, DTA, (%/°C) are given. The TGA curve indicates that the weight loss of precursors has occurred from 40 to 360 °C, suggesting that the precursors decomposed completely to become nickel oxide below 360 °C. Two distinct intervals of weight loss were observed in the TGA curves, accompanied by two peaks of the weight loss rate in the DTA curves. The first peak of weight loss rate located between 40 and 87 °C may be attributed to the thermal dehydration of the precursors and the evaporation of the physically absorbed water, and the corresponding weight loss was 9.2%. The second peak of weight loss rate located between 263 and 356 °C may be related to the decomposition of nickel hydroxide in the precursors accompanying a weight loss of 15.3%.

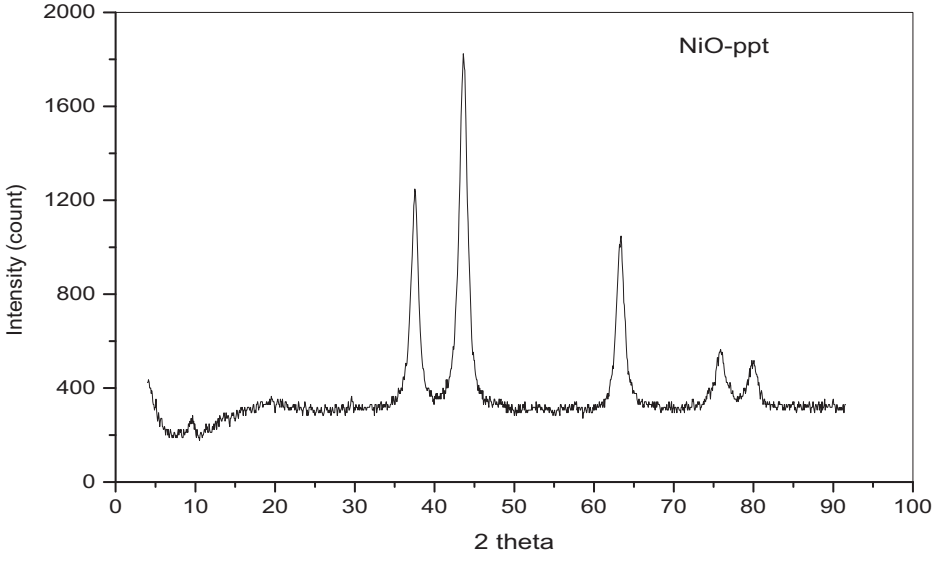


**Figure 1** X-ray diffraction of the sample prepared by the precipitation method.

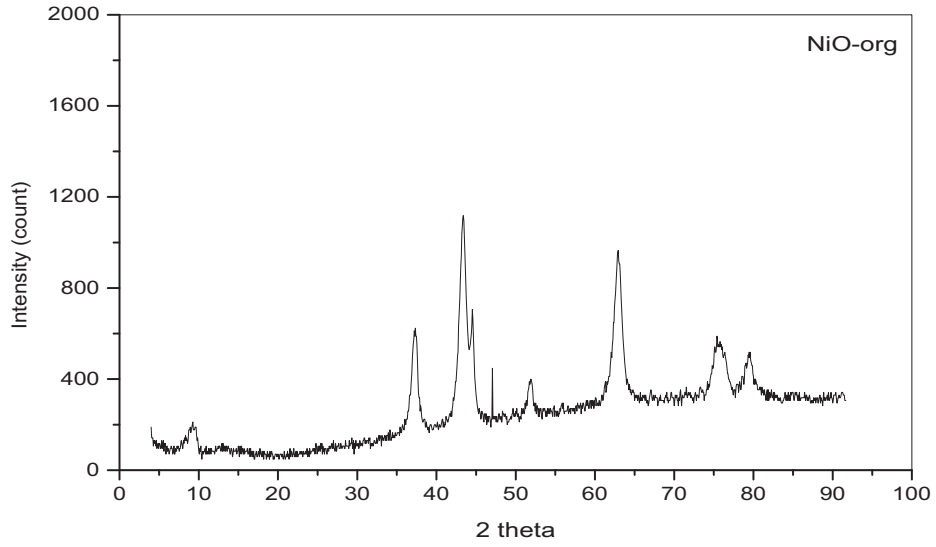


**Figure 2** X-ray diffraction of the sample prepared by the organic solvent method.

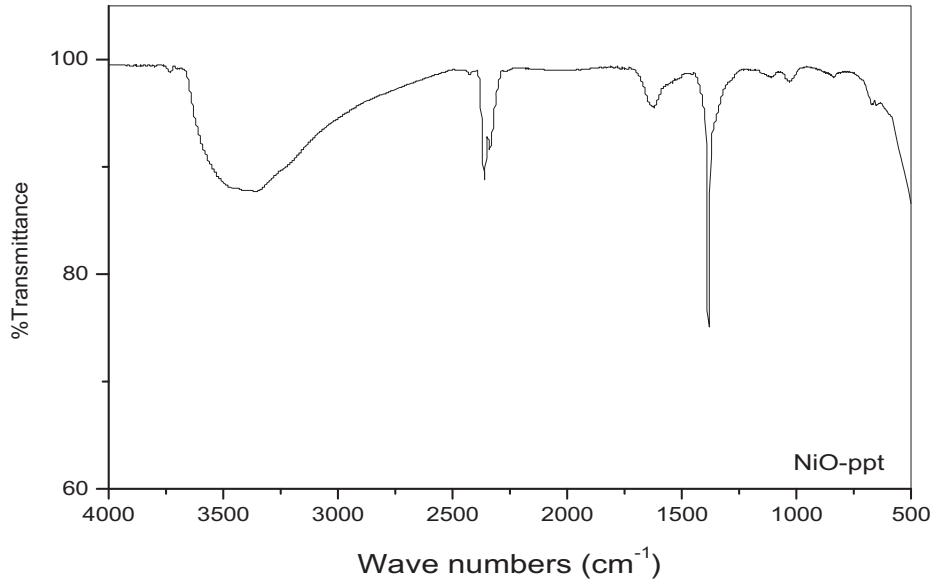


**Figure 3** FTIR Spectra of nickel oxide catalyst prepared by the precipitation method.

### *3.1.4. Surface and textural analyses*

The $N_2$ adsorption–desorption isotherms of the NiO prepared by precipitation and organic method ($NiO_{ppt}$, $NiO_{org}$) catalysts are shown in Fig. 6. It can be seen that, a near type II isotherm with hysteresis loops, characteristic of macro porous materials according to the IUPAC classification was obtained. The textural properties of the two catalysts are summarized in Table 1. It can be noted that the specific surface area and total pore volume of the $NiO_{org}$ catalyst are larger than those of the $NiO_{ppt}$ catalyst. The high surface area of $NiO_{org}$ catalyst than that of $NiO_{ppt}$ catalyst suggests that the organic method has aided to form smaller particles of the active NiO species due to an induced interaction through the preparation method employed, which is indicated further from the average pore size which is proved to be smaller for $NiO_{org}$ than $NiO_{ppt}$, Table 1 [24].

### *3.2. Effect of contact time*

The effect of the contact time of removal of Pb(II) ions by $NiO_{ppt}$ and $NiO_{org}$ is shown in Fig. 7. The equilibrium was attained after shaking for 120 min, which is considered as adequate and economical for wastewater treatment plant application [25]. According to these results, the agitation time was fixed at 2 h for the rest of the batch experiments to make sure that equilibrium was attained [23].

### *3.3. Effect of adsorbent mass*

The effect of adsorbent quantity of removal of Pb(II) is presented in Fig. 8. The results indicate that the adsorption of Pb ions increases with increasing NiO mass up to a certain

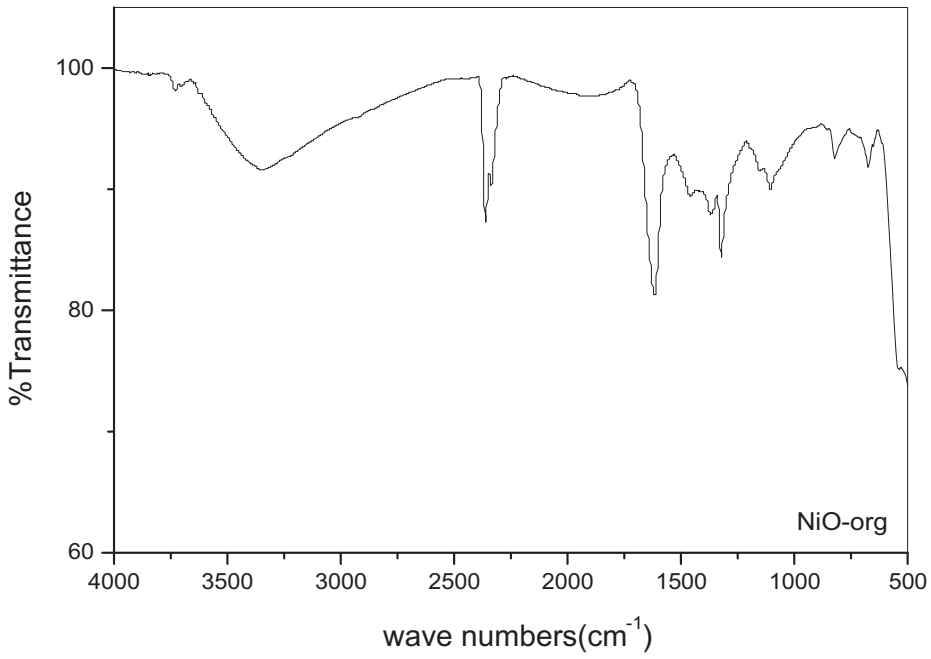


**Figure 4** FTIR Spectra of nickel oxide catalyst prepared by the organic solvent method.

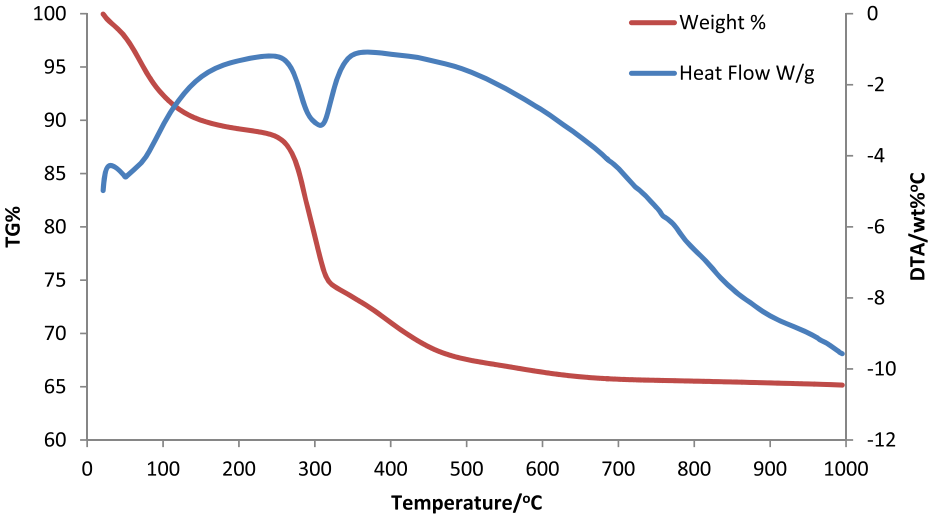


**Figure 5** TG–DTA curves of the precursor.

value and then becomes almost constant. Therefore, the optimum no quantities were selected from 0.025 g to 25 ml of Pb(II) solution. It is apparent that the percent removal of Pb(II) increases by the increase of the NiO concentration due to the availability of the exchangeable active sites of the NiO adsorbent particles [26,27].

### *3.4. Effect of initial concentration of heavy metal*

The effect of initial concentration on the percentage removal of Pb(II) by $NiO_{ppt}$ and $NiO_{org}$ is shown in Fig. 9. It can be seen from the results that the percentage removal decreases with the increase in initial concentration, where it is seen that the adsorption of Pb(II) decreased gradually from 100% to 29% for $NiO_{ppt}$ and from 100% to 68% for $NiO_{org}$ upon increasing the Pb(II) concentration of 5 mg/L to 100 mg/L, respectively. Sufficient adsorption sites are available at lower initial concentrations, but at higher concentrations metal ions are greater than adsorption sites. Thus, it can be said that removal of lead is concentration dependent using nano NiO particles as previously reported [28,29].

### *3.5. Adsorption isotherms*

The fitted constants for Freundlich and Langmuir models along with regression coefficients are summarized in Table 2 configured from the graphic Figs. 10 and 11. As can be seen from isotherms and regression coefficients, the fit is better with

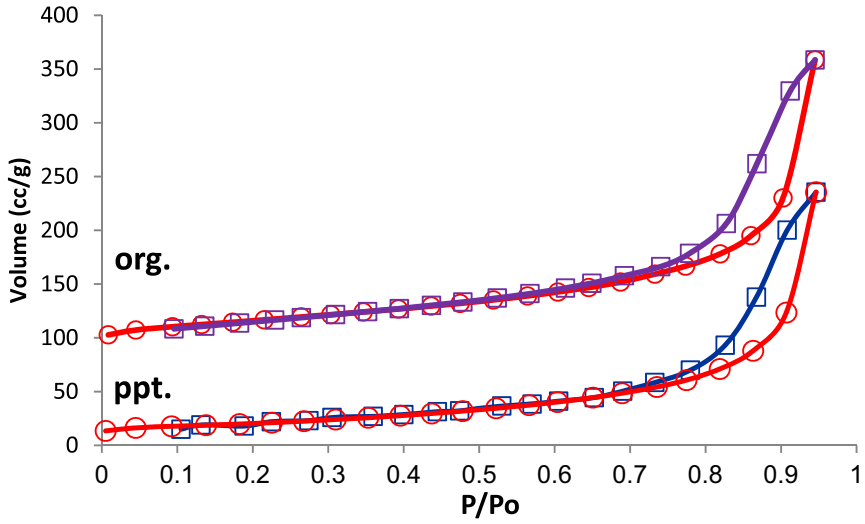


**Figure 6** $N_2$ isothermal adsorption and desorption profiles over NiO-org than NiO-ppt catalysts.

**Table 1** Textural parameters of NiO-org and NiO-ppt catalysts.

| Textural parameters | Catalysts | |
|---|---|---|
| | Ni-oxide (ppt.) | Ni-oxide (org.) |
| Surface area, $m^2/g$ | 72.505 | 128.330 |
| Total pore volume, cc/g | 0.364 | 0.431 |
| Average pore size, Å | 100.48 | 67.12 |
| Average pore size, nm | 10.05 | 6.71 |

Langmuir model than with Freundlich model. Langmuir constant $q_m$ was 56.24297 mg/g and 21.54708 mg/g for Pb(II) ion uptake by $NiO_{org}$ and $NiO_{ppt}$, respectively. Such conclusion indicates clearly the sorption limitation of the Pb ions by the NiO particles and as evidences from sorption data.

### 3.6. Adsorption kinetics

Fig. 12, describes the rate of removal of $Pb^{+2}$ ion as very fast with its disappearance from the solution sharply in the first 20 min. After 2hours, $Pb^{+2}$ ion residual concentration was about 3.57 and 27.9 ppm by $NiO_{ppt}$ and $NiO_{org}$ catalysts, respectively indicating that $NiO_{org}$ catalyst acquire relatively large surface area (Table 1) and strong adsorption capacity than $NiO_{ppt}$ catalyst [30] (Fig. 13).

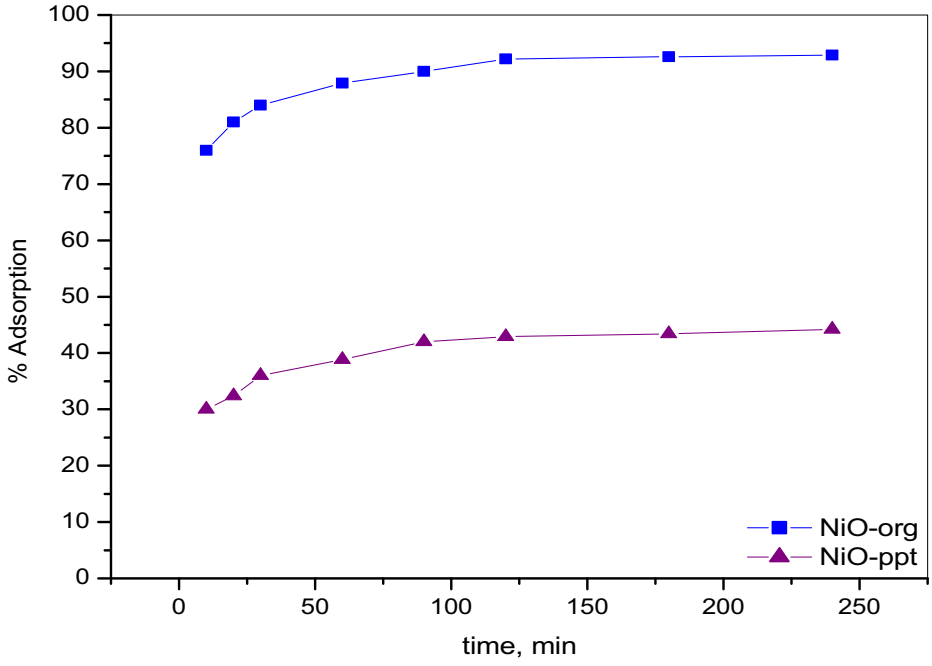


**Figure 7** Effect of contact time on adsorption of Pb(II) (initial concentration 50 mg/L, 0.025 g NiO-ppt and NiO-org/25 ml solution, initial pH of solution 5.8, temp., 298 K).

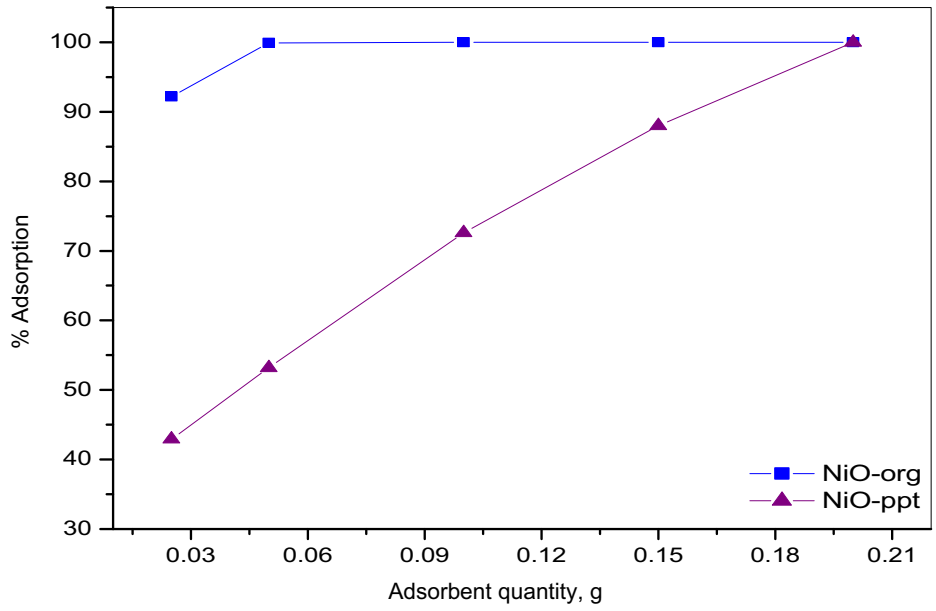


**Figure 8** Effect of adsorbent quantity on Pb(II) removal for NiO (initial concentration 50 mg/L, initial pH of solution 5.8, contact time 120 min, temp 298 K).

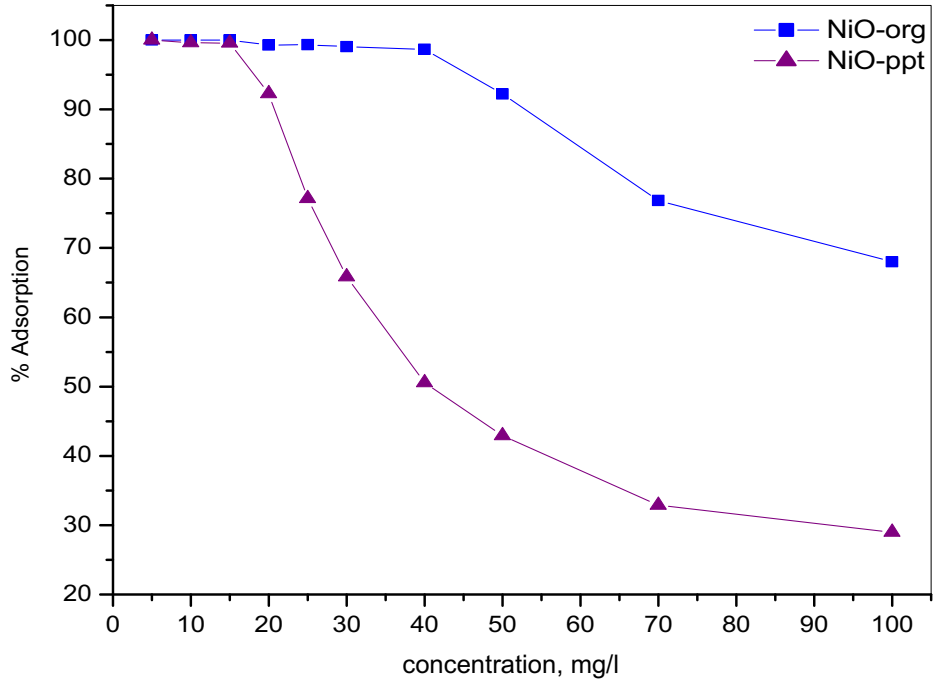


**Figure 9** Effect of initial concentration on adsorption of Pb(II) (contact time 120 min., 0.025 g/25 mL solution, initial pH of solution 5.8, temp., 298 K).

**Table 2** Isotherm constants of Langmuir and Freundlich models for Pb(II) ions uptake by NiO-org and NiO-ppt.

| Adsorbent | Langmuir constants | | | Freundlich constants | | |
|---|---|---|---|---|---|---|
| | $q_m$ (mg/g) | $k_L$ (L/mg) | $R^2$ | $k_F$ | $n$ | $R^2$ |
| NiO-org | 56.24297 | 4.21327 | 0.9799 | 1.5355 | 0.646275 | 0.95136 |
| NiO- ppt | 21.54708 | 23.8 | 0.93683 | 1.258577 | 0.824436 | 0.92262 |

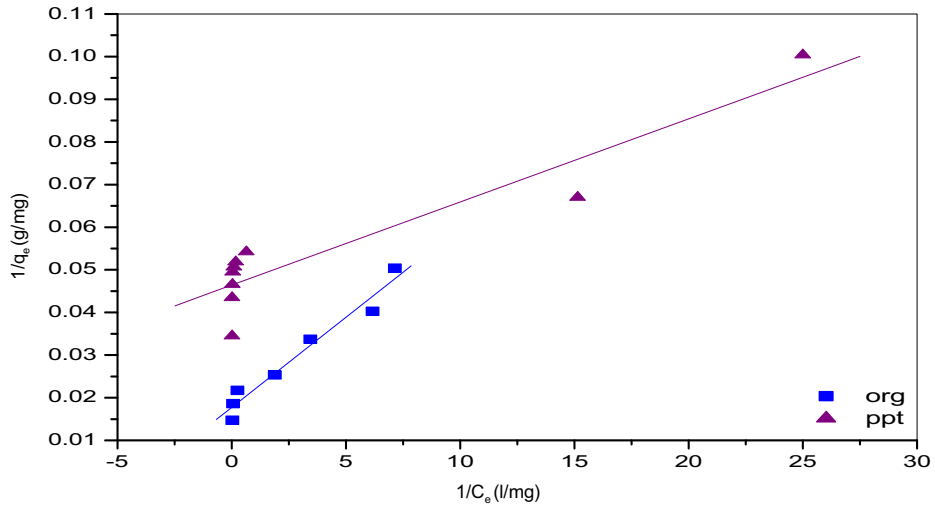


**Figure 10** Langmuir isotherm plot for adsorption of Pb(II) onto NiO.

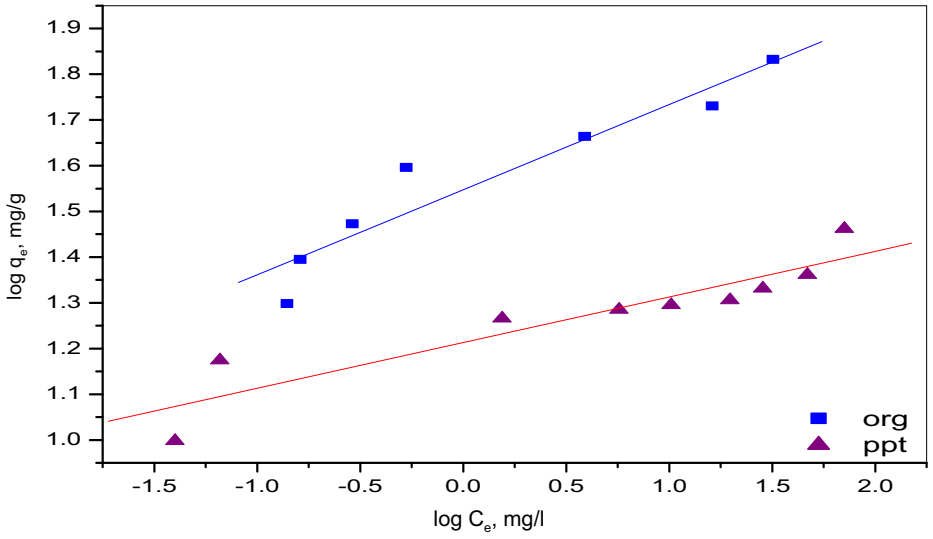


**Figure 11** Freundlich isotherm plot for adsorption of Pb(II) onto NiO.

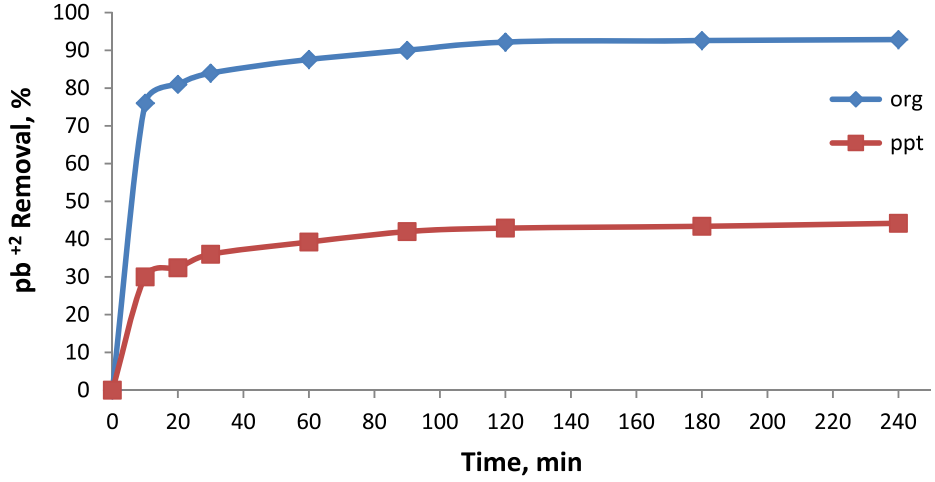


**Figure 12** Concentration variation of $Pb^{+2}$ ion with time.

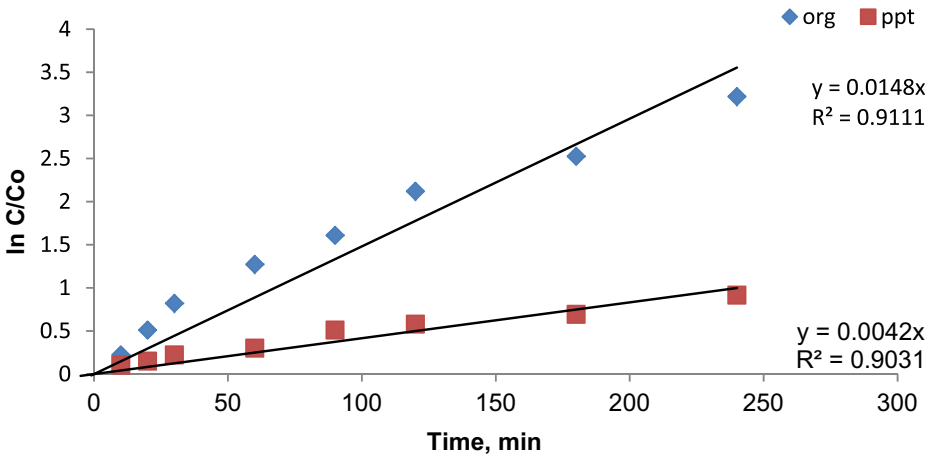


**Figure 13** Relationship between logarithmic plots of $Pb^{+2}$ ion concentration versus time.

After 2 h of reaction the residual concentration of $Pb^{+2}$ ion in solution was below the detection limit, the logarithmic plots of residual concentration of $pb^{+2}$ ion in solutions versus time, show good linear relationship and the correlation coefficient ($R^2$) is larger than 0.9. It may be concluded that the rate of $Pb^{+2}$ ion concentration reduction by $NiO_{ppt}$ and $NiO_{org}$ catalysts can be described by the pseudo first-order reaction.

## 4. Conclusions

The present study shows that NiO-nanoparticles prepared by the organic solvent method is more active than that prepared by the precipitation method for removal of Pb(II) ions from aqueous solutions. The adsorption process is a function of the adsorbent and adsorbate concentrations and contact time. Equilibrium was achieved practically in 2 h. Langmuir model is found to be in a good agreement with experimental data on adaptive behavior of Pb(II) ions on NiO. Nickel oxide is then considered as a useful catalyst for the treatment of wastewater containing lead.

## References

[1] M. Jamil, M.S. Zia, M. Qasim, J. Chem. Soc. Pak. 32 (2010) 370–378.
[2] S. Khan, Q. Cao, Y.M. Zheng, Y.Z. Huang, Y.G. Zhu, Environ. Pollut. 152 (2008) 686–692.
[3] A. Singh, R.K. Sharma, M. Agrawal, F.M. Marshall, Food Chem. Toxicol. 48 (2010) 611–619.
[4] S.H. Peng, W.X. Wang, X.D. Li, Y.F. Yen, Chemosphere 57 (2004) 839–851.
[5] Guidelines for Drinking-Water Quality, 2nd ed., Vol. 1, World Health Organization, Geneva, 1998.
[6] F.L. Fu, Q. Wang, J. Environ. Manage. 92 (2011) 407–418.
[7] Y.H. Wang, S.H. Lin, R.S. Juang, J. Hazard. Mater. 102 (2003) 291–302.
[8] D.W. O'Connell, C. Birkinshaw, T.F. O'Dwyer, Bioresour. Technol. 99 (2008) 6709–6724.
[9] T.A. Kurniawan, G.Y.S. Chan, W.H. Lo, S. Babel, J. Chem. Eng. 118 (2006) 83–98.
[10] N. Galil, M. Rebhun, Water Sci. Technol. 22 (1990) 203–210.
[11] M. Eid, A.M.A. Omar, A.M. Dessouki, Recovery of Chromium Ions From Electroplating Wastewater by Flotation Gamma Irradiation and Adsorption onto Hydrogels, 8th Arab International Conference On Polymer Science & Technology, 27–30 November, Cairo-Sharm El-Shiekh, EGYPT (2005).
[12] B.J. Pan, B.C. Pan, W.M. Zhang, L. Lv, Q.X. Zhang, S.R. Zheng, J. Chem. Eng. 151 (2009) 19–29.
[13] S.P. Mishra, V.K. Singh, D. Tiwari, Appl. Radiat. Isot. 47 (1996) 15–21.
[14] J.E. Vanbenschoten, B.E. Reed, M.R. Matsumoto, P.J. McGarvey, J. Water Environ. Res. 66 (1994) 168–174.
[15] J.A. Coston, C.C. Fuller, J.A. Davis, Geochim. Cosmochim. Acta 59 (1995) 3535–3547.
[16] A. Agrawal, K.K. Sahu, J. Hazard. Mater. 137 (2006) 915–924.
[17] M. El, S. Abd el Raouf, A.M. Abd El Raheim, A.F. El Kafrawy, N. El, S. Maysour, A.Kh. Ibraheim, A.A. Abdel, Int. J. Chem. Mater. Sci. 2 (2013) 036–044.
[18] G.-J. Li, X.-X. Huang, Y. Shi, J.-K. Guo, J. Mater. Lett. 51 (2001) 325–330.
[19] A. Imtiaz, U. Rafique, J. Int. Chem. Environ. Eng. 2 (6) (2011).
[20] S. Rengaraj, C.K. Joo, Y. Kim, J. Yi, J. Hazard. Mater. B 102 (2003) 257–275.
[21] S.V. Ganachari, R. Bhat, R. Deshpande, A. Venkataraman, Recent Res. Sci. Technol. 4 (4) (2012) 50–53.
[22] Z.-F. Zhao, Z.-J. Wu, L.-X. Zhou, M.-H. Zhang, W. Li, K.-Y. Tao, Catal. Commun. 9 (2008) 2191–2194.
[23] M.N. Rifaya, T. Theivasanthi, M. Alagar, Chemical Capping Synthesis of Nickel Oxide Nanoparticles and their Characterizations Studies, Center for Research and Post Graduate Department of Physics, Ayya Nadar Janaki Ammal College, Sivakasi – 626124, Tamilnadu, India, 2010.
[24] F.Y.A. El Kady, M.G. Abd El Wahed, S. Shaban, A.O. Abo El Naga, J. Fuel 89 (2010) 3193–3206.
[25] K. Kadirvelu, C. Namasivayam, Activated carbon from coconut coirpith as metal adsorbent: adsorption of Cd (II) from aqueous solution, Adv. Environ. Res. 7 (2003) 471–478.
[26] B. Muhammad, Ibrahim, Wahab L.O. Jimoh, Int. J. Biol. Chem. Sci. 5 (3) (2011) 915–922.
[27] Y. Feng, J.-L. Gong, G.-M. Zeng, Q.-Y. Niu, H.-Y. Zhang, C.-G. Niu, J.-H. Deng, M. Yan, Chem. Eng. J. 162 (2010) 487–494.
[28] M.M. Rao, A. Ramesh, G.P.C. Rao, K. Seshaiah, J. Hazard. Mater. B129 (2006) 123–129.
[29] F.I. Abdel Samea, S.A. Shaban, N.A. Yussef, M.M. Selim, Egypt. J. Pet. 19 (1) (2010).
[30] O.A. Fadali, E.E. Ebrahiem, Y.H. Magdy, A.A. Daifullah, M. Nassar, J. Environ. Sci. Health Part A Environ. Sci. Eng. 9 (2005) 465–472.